Research paper

Experimental observation of flow characteristics over a Piano Key Weir

OLIVIER MACHIELS, PhD Student, *HACH, ArGEnCo department, University of Liege, Chemin des chevreuils 1 B52/3, 4000 Liege, Belgium.*
*Fund for education to Industrial and Agricultural Research.
Email: OMachiels@ulg.ac.be (author for correspondence)

SEBASTIEN ERPICUM (IAHR Member), PhD, *HACH, ArGEnCo department, University of Liege, Chemin des chevreuils 1 B52/3, 4000 Liege, Belgium.*
Email: S.Erpicum@ulg.ac.be

BENJAMIN J. DEWALS, (IAHR Member), PhD, *HACH, ArGEnCo department, University of Liege, Chemin des chevreuils 1 B52/3, 4000 Liege, Belgium.*
*Belgian Fund for Scientific Research F.R.S.-FNRS
Email: B.Dewals@ulg.ac.be

PIERRE ARCHAMBEAU, PhD, *HACH, ArGEnCo department, University of Liege, Chemin des chevreuils 1 B52/3, 4000 Liege, Belgium.*
Email: Pierre.Archambeau@ulg.ac.be

MICHEL PIROTTON (IAHR Member), *Professor, HACH, ArGEnCo department, University of Liege, Chemin des chevreuils 1 B52/3, 4000 Liege, Belgium.*
Email: Michel.Pirotton@ulg.ac.be

ABSTRACT
The Piano Key Weir is a type of labyrinth weir using overhangs to reduce the footprint of the foundation. These are directly placed on a dam crest. Together with its high discharge capacity for low heads, this geometry makes these weirs interesting in dam rehabilitation. However, the Piano Key Weir is a new weir type, first designed in 2001 and built from 2006 by Electricité de France. Even though experimental studies confirmed its appealing discharge capacities, the flow upstream, over and downstream of this complex structure is still not well known. This research presents experimental test results performed on a 1:10 scale model. The experiments aim at determining the flow features along the weir depending on the upstream head. The flow conditions are characterized in terms of specific discharge, velocity, pressure, water level and streamlines along the weir.

Keywords: Free surface flow, physical model, Piano Key Weir, pressure distribution, streamline, velocity distribution

1 Introduction

The Piano Key Weir (PKW) is a novel weir type developed by Blanc and Lempérière (2001) and Lempérière and Ouamane (2003) to combine the benefits of a labyrinth weir with overhangs to facilitate the weir location on a dam crest. The first-scale model studies indicated that this weir is up to four times more efficient than a traditional ogee-crested weir at an equal head and crest length (Ouamane and Lempérière 2006a).

The PKW has a particular geometry including up- and/or downstream overhangs of variable width, in- and outlet bottom slopes, involving a large set of geometric parameters (Fig. 1). The "PKW-unit" is the basic structure of a PKW, composed of two transversal walls, an inlet and two half outlets. Its main geometric parameters are weir height P, the number of PKW-units N_u, lateral crest length B, in- and outlet widths W_i and W_o, up- and downstream overhang lengths B_o and B_i and the wall thickness T_s (Pralong *et al.* 2011).
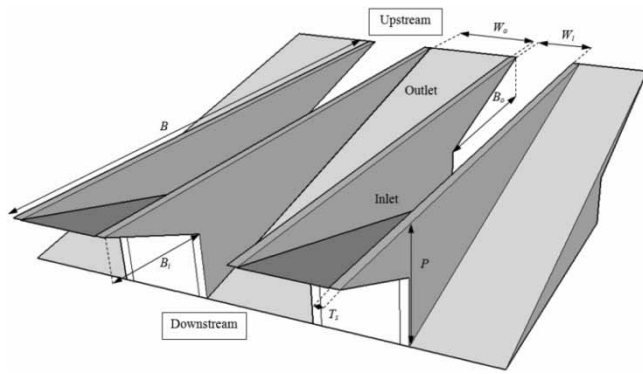
Figure 1   3D sketch of PKW with main geometric parameters

Experimental studies have been carried out to characterize the effect of these geometrical parameters on the discharge capacity (Hien *et al.* 2006, Ouamane and Lempérière 2006b, Le Doucen *et al.* 2009, Machiels *et al.* 2009a). Increasing the inlet/outlet width ratio W_i/W_o, the upstream overhang length B_o and the weir height P were considered to optimize the discharge capacity (Ouamane and Lempérière 2006b, Le Doucen *et al.* 2009). The shape of the upstream overhang also contributes to the discharge capacity. Hien *et al.* (2006) or Ouamane and Lempérière (2006a) analyzed the performance of a PKW in view of the aeration capacity and floating debris passage.

The first prototype size PKW was built by 'Electricité de France' (EDF) during 2006 to increase the discharge capacity of the Goulours Dam spillway (Laugier 2007). Based on good experience and additional scale model tests, EDF favoured the use of PKW in dam rehabilitation in France. Two PKWs were

built on St. Marc and Gloriettes Dams in 2008 and 2009 (Bieri *et al.* 2009, Laugier *et al.* 2009).

Based on the first experimentation, numerical models have also been developed. A 3D model was used by EDF to design project models then tested in laboratories (Luck *et al.* 2009). Based on the current knowledge of the flow features over a PKW, a 1D model was developed at the University of Liège to improve its design by parametric studies (Erpicum *et al.* 2010).

The current hydraulic design of a PKW is performed based on scale model studies, modifying step-by-step an initial geometry proposed by project engineers (Leite Ribeiro *et al.* 2007). There is thus a strong need for fundamental as well as applied studies on the PKW to improve the understanding of its flow features and to set up efficient design rules to predict its discharge capacity. Therefore, a combined experimental and numerical study, exploiting advantages of the two methods, was undertaken at the Laboratory of Engineering Hydraulics, University of Liège, as successfully adopted previously by Fraccarollo and Toro (1995), Capart *et al.* (1997) and Muste *et al.* (2001). The principle aim of this study is to enhance the understanding of the flow physics on a PKW to define its benefits and limitations.

2   Experimental setup

A steel test channel 7.2 m long, 1.2 m wide and 1.2 m high was built to perform the scale model tests (Fig. 2). It was fed by up to 300 l/s. The channel intake was equipped with a metal grid and a synthetic membrane ensuring uniform flow conditions. Two
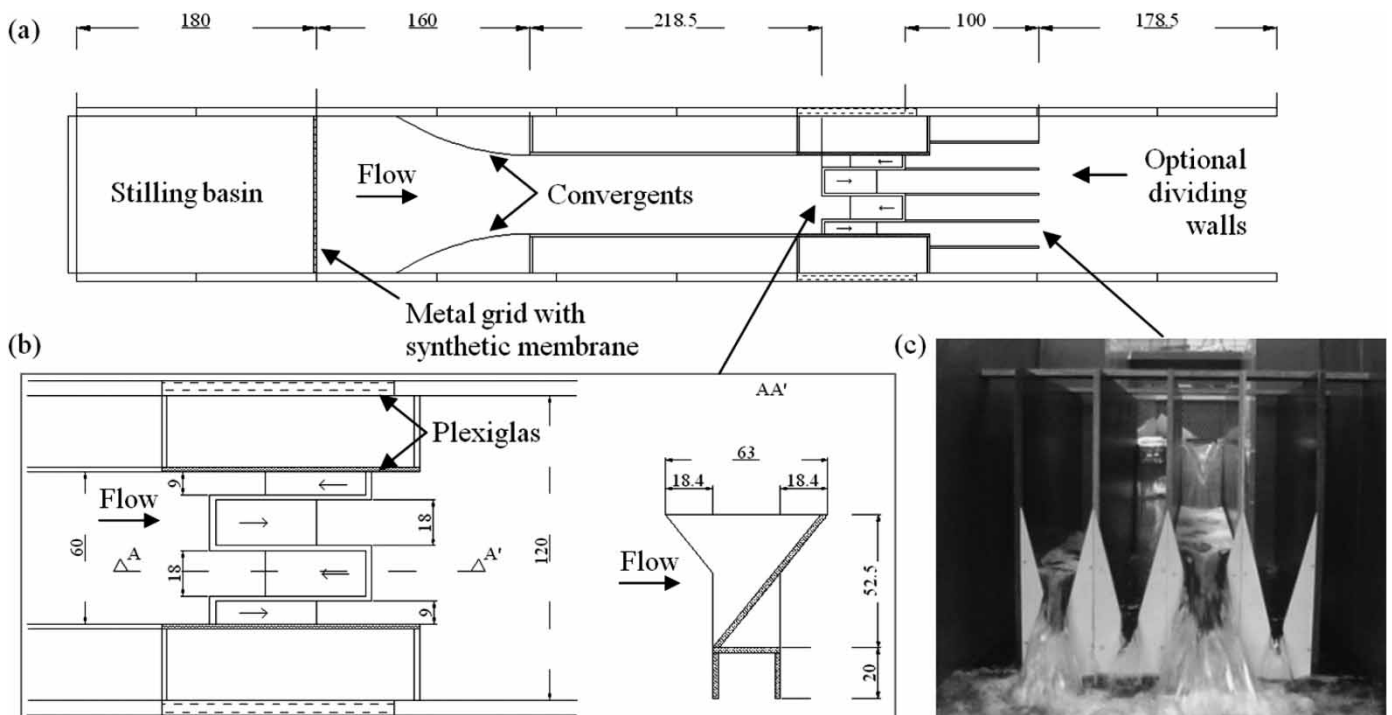

Figure 2   Test set-up (a) plan of channel, (b) plan of PKW model and (c) optional sharp-crested triangular weirs (length in cm)

Plexiglas plates on both channel sides allowed us to observe the flow patterns of the PKW model. Convergent walls reduced the channel width to that of the test model.

A 1:10 scale model of basic PKW geometry (Fig. 2) was used to investigate the flow features on the weir crests and to characterize discharge, velocity, pressure and flow patterns. The test model included 1.5 inlets and 1.5 outlets, of which the halves allowed us to observe the flow, while the full widths at the channel centre permitted measurements without side effects, as discussed below.

Discharge and upstream flow depth data were taken with an electromagnetic flow meter and a gauge of ± 1 l/s and ± 0.5 mm reading accuracies, respectively. Streamline observations upstream of the weir and in the inlets were made using coloring fluoresceine dye for selected tests. The dye was supplied 0.38 m upstream of the weir basis, at heights 0.05, 0.25, 0.55, 0.75 and 0.8 m above the channel bottom and at 0.045, 0.2, 0.3, 0.4 and 0.555 m from the left side of the channel (Fig. 3).

Six Pitot tubes (Klopfenstein 1998) and a Vernier gauge were used to take velocity, pressure and free surface data of ± 0.5 mm reading accuracy. The Pitot tubes were placed on the channel to measure flow velocity and pressure head at various heights and locations upstream of the weir. Their reading accuracy is ± 1 mm, corresponding to ± 0.15 m/s for velocity. These measurements were made at 0.11, 0.32, 0.53 and 0.74 m upstream of the downstream PKW crest over the entire channel width spaced 3.3 cm at elevations 0.05, 0.25, 0.55 and 0.75 m from the channel bottom, resulting in a total of 117 measurement points (Fig. 3).

Discharge measurements were made downstream of the inlet, the outlet and both the half-inlet and -outlet using separated

Figure 3   (cross symbols) Dye supply and (filled circles) Pitot measurement locations (a) plan and (b) inlet section (length in cm)

channels and triangular weirs. The downstream channel was divided into four rectangular portions ending with triangular sharp-crested weirs (Fig. 2). Wooden plates of 1.5 cm thickness were used for channel division to limit the effect of wall thickness on the discharge capacity. The discharges in the four channels were determined based on CETMEF (2005). The sum of the calculated partial discharges agreed better than 5.5% of the totally measured upstream discharge.

3   Results

3.1   *Discharge capacity*

Because of the complexity of a PKW geometry, the discharge Q was expressed with a common weir equation involving the head H on the weir versus the weir length W as

$$Q = C_{dW} W \sqrt{2gH^3} \qquad (1)$$

where (Fig. 2)

$$W = 1.5(W_i + W_o) + 3T_s \qquad (2)$$

The effect of weir geometry is thus lumped into the discharge coefficient C_{dW} (Ouamane and Lempérière 2006a). The non-dimensional model discharge/head curve was measured over a wide range of discharges (Fig. 4) with error bars indicating the effect of measurement accuracy. Regions A and B are the decreasing and stabilization regions, respectively, as described above.

The partial discharges downstream of the model indicate the side wall effect. Its effect on the downstream crest is highlighted by comparing the discharges downstream of the full and half inlets. To isolate the effects of the lateral and the upstream crests, full and half outlet discharges were measured with and without the upstream crest closed, using a PVC plate to raise the upstream crest level over the free surface. This caused less than 1% of the discharge curve downstream of the inlet, suggesting a similar discharge distribution with and without the PVC plate.

The discharge over the downstream crest increases up to 15% with the presence of a side wall. Considering the outlets without the upstream crests, the discharge is almost unaffected by the side walls as compared with discharge accuracy (<5% difference between half and full outlets). The discharge of the lateral crest is thus similar for a complete and a half outlet, confirming flow symmetry along the outlet axis. The discharge of the half-outlet decreases by 15% as compared to the full outlet, which is directly linked to discharge reduction on the upstream crest.

A comparison between combined discharges of the full-inlet and -outlet with the combined discharges of the two half-inlet and -outlet indicates differences of ~ 1 l/s, corresponding to the flow meter accuracy. The discharge increase in the half-inlet is thus counterbalanced by a decrease in the half-outlet. The head/discharge curve of Fig. 4, considering 1.5 PKW-units,
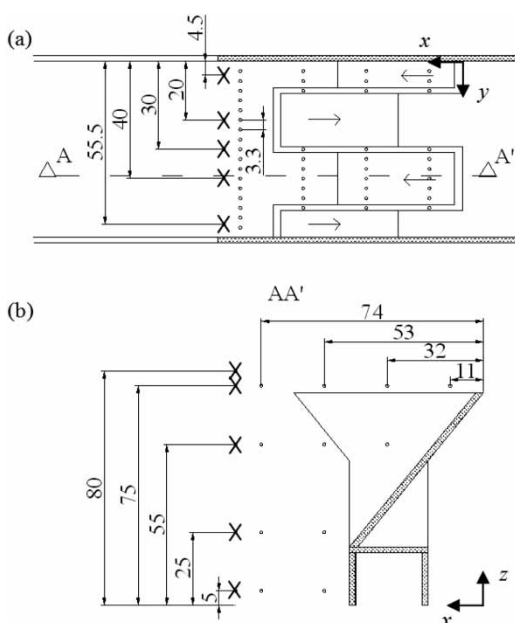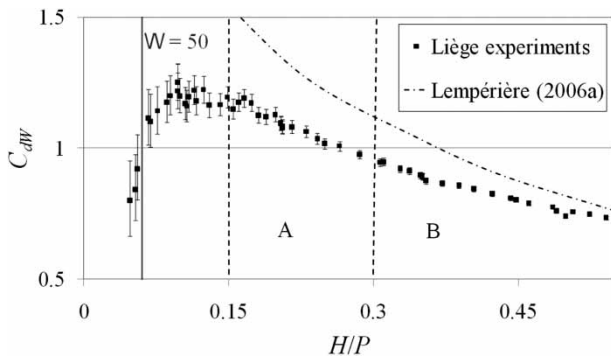
Figure 4   Non-dimensional head/discharge relation of Liège tests ($L/W = 4.15$, $W_i/W_o = 1$, $W_u/P = 0.76$, $B_o/B_i = 1$) and Lempérière (2006a) tests ($L/W = 4$, $W_i/W_o = 1$, $W_u/P = 1.1$, $B_o/B_i = 1$) with decreasing region A and stabilization region B, (vertical line) limit of surface tension effects $W = 50$

allows thus to represent discharge over a similar PKW for any number of units, thus justifying a limited number of PKW-units. These results agree with those of Le Doucen *et al.* (2009) and Luck *et al.* (2009).

3.2   *Low head behaviour*

For low heads, the transition from a partially clinging nappe to a leaping nappe and then to a springing nappe flow (Johnson 2000) is observed on the various portions of the PKW crest. These transitions occur for rising head, depending on crest thickness T_s and crest shape. A 2 cm thick lateral crest thickness, and up- and downstream crest thickness of 2.4 cm were used because of the slope of the PVC plates (Fig. 2).

On the lateral crests, for the smallest head ratio of $H/P = 0.05$, the leaping nappe remains in contact with the crest. For $0.09 \leq H/P \leq 0.10$, corresponding to $2.35 \leq H/T_s \leq 2.6$, the nappe starts springing free and is detached from the crest along the downstream crest portion (Machiels *et al.* 2009b), a situation which persists for higher heads. The same behavior occurs on the downstream inlet crest. The transition from leaping to springing nappe occurs for $0.11 \leq H/P \leq 0.12$, corresponding to $2.4 \leq H/T_s \leq 2.6$ (Machiels *et al.* 2009b). Since identical transitions are observed for the same H/T_s ratios on the lateral and the downstream crests, the inlet slope seems to have no effect on the nappe shape for low heads.

The flow behaviour on the upstream crest is different from that on the downstream and lateral crests. For the lowest head ratios, the nappe is completely attached to the walls. Then for $0.16 \leq H/P \leq 0.17$, i.e. $3.5 \leq H/T_s \leq 3.6$, the nappe is fully aerated (Machiels *et al.* 2009b). The downstream outlet slope has thus a significant effect on the nappe shape, delaying the transition to the springing nappe for higher H/T_s ratios.

3.3   *Streamlines*

The streamlines were determined for 12 heads, ranging from $H/P = 0.05$ to 0.45. For low heads ($H/P \leq 0.2$), the streamlines
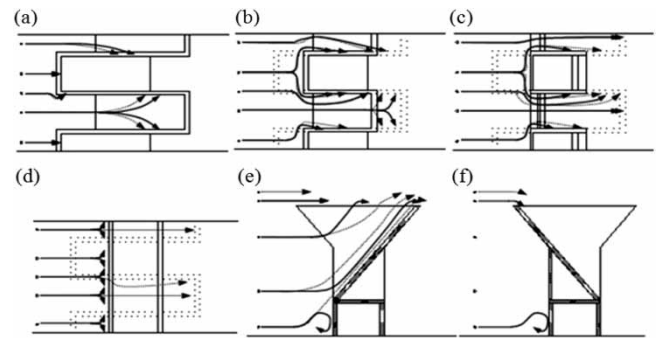

Figure 5   Streamlines for (dashed arrow) low ($H/P \leq 0.2$) and (dash-dashed arrow) high heads ($H/P > 0.2$) at different weir heights for z (cm) = (a) 72.5, (b) 55, (c) 25, (d) 5 and along (e) inlet, (f) outlet

are homogeneously distributed along the entire weir crest. The downstream inlet crest is mainly supplied from the bottom current, whereas the upstream outlet crest is mainly supplied from the surface current. The lateral crest is supplied in its downstream portion by the front inlet current and on its upstream part by the front outlet current, originating under the crest level (Fig. 5). For $H/P > 0.2$, the streamline distribution appears less optimal. The downstream inlet crest is supplied by the bottom current and also by the front inlet current. The upstream outlet crest still supplied by the surface current, whereas the lateral crest is poorly supplied from the front outlet current, coming under the crest level (Fig. 5). The transition between these streamline sketches corresponds to the transition from flat to undular free surface profiles (Fig. 6).

3.4   *Free surface, velocity and pressure head profiles*

Free surface, velocity and pressure profiles were measured upstream of the weir and along the inlet for $H/P = 0.1$ (low head), 0.2 (transition head) and 0.35 and 0.5 (high head). The free surface profiles confirm the transition between a flat-free surface along the inlet for $H/P = 0.1$ to undular flow for $H/P = 0.35$ (Fig.7).

The pressure head profiles are close to hydrostatic distribution along the side wall and along the inlet centre except for locations of dense streamlines (Fig. 5), where an over-pressure zone occurs, as also in front of the angles near the inlet entrance (Machiels *et al.* 2010). This over-pressure increases with the upstream head.
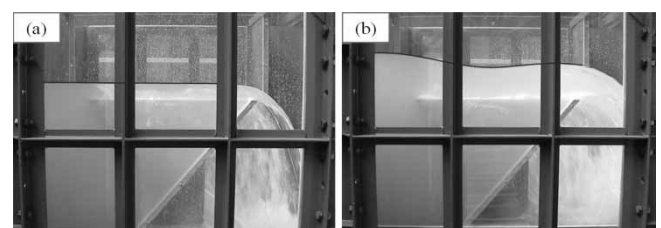

Figure 6   Free surface profiles for low and high heads of $H/P =$ (a) 0.15 and (b) 0.35
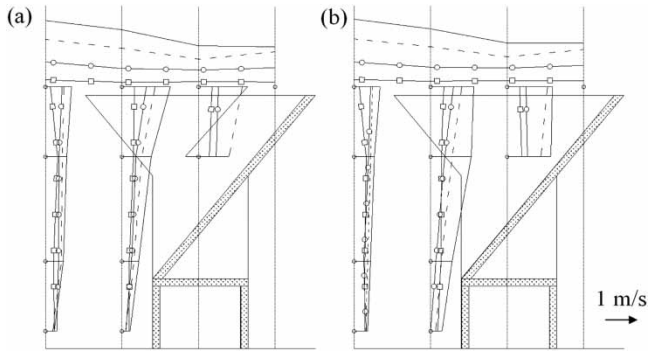
Figure 7　Free surface and velocity profiles (a) near side wall ($y = 0.467$ m) and (b) inlet centre ($y = 0.4$ m) for $H/P =$ (thin line) 0.5, (dashed line) 0.35, (dashed line with circle) 0.2, (dashed line with vertical line) 0.1

The velocity profiles for $H/P = 0.1$ and 0.2 are relatively uniform along the side wall and the inlet centre (Figs. 7 and 8), as is illustrated by the homogeneous streamline distribution. For $H/P = 0.35$ and 0.5, the velocity increases along the inlet centre (Figs. 7b and 8). The closer the measurement point from the downstream crest, the higher the velocity, illustrating a streamline concentration. For $H/P = 0.5$, negative velocities are observed near the side walls downstream of the inlet entrance (Figs. 7a and 8).

4　Discussion

The non-dimensional discharge/head curve of Fig. 4 is similar to that found in Ouamane and Lempérière (2006a) for poor PKW characteristics. The model geometry was defined to emphasize the differences between various weir flow types by increasing the slopes of both inlets and outlets, thus globally decreasing the PKW efficiency. For low heads ($H/P < 0.15$), there is an important reduction in the discharge coefficient as compared to Lempérière's results (Fig. 4) because of the effects of thickness and shape of the crest. Lempérière's model was made with thin steel plates (2 mm), whereas the present model had PVC plates of 2 cm thickness.

For $H/P < 0.06$, the Weber number

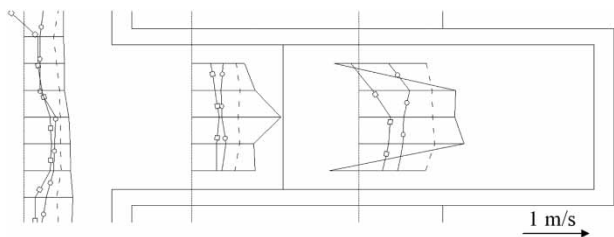$$W = \frac{\rho U^2 H}{\sigma} \tag{3}$$

Figure 8　Velocity profiles along inlet at $z = 0.55$ m for $H/P =$ (thin line) 0.5, (dashed line) 0.35, (thin line with circle) 0.2, (thin line with open square) 0.1

where ρ is the water density, σ the surface tension and U the flow velocity (<50), and surface tension effects may become significant, therefore (Novak *et al.* 1990). Johnson (2000) demonstrated that the transition from a leaping nappe to a springing nappe occurs for $1.8 \leq H/T_s \leq 3$, depending on the weir dimensions. The smaller are the weir dimensions, the more important is H/T_s at the transition. These values agree with these for the transition on the lateral and the downstream crests (§3.2). Regarding weir efficiency, Johnson also stated that this transition is in-line with a slope variation of the non-dimensional discharge/head curve.

Swamee (1988) proposed a formulation of the discharge coefficient C_{dL} for linear weirs with the finite crest thickness. His formulation is in agreement with the observation of the transition from the steep-slope of the C_{dL}-curve for heads corresponding with a leaping nappe to a low-slope for heads corresponding with a springing nappe, namely

$$
\begin{aligned}
C_{dL} &= \frac{3}{2} C_{dW} \frac{W}{L} \\
&= 1.06 \left\{ \begin{array}{l} \left(\dfrac{14.14}{8.15 + \chi}\right)^{10} + \left(\dfrac{\chi}{\chi + 1}\right)^{15} \\[2mm] + 1.834 \left[1 + 0.2\left(\dfrac{\gamma^5 + 1.5\gamma^{13}}{1 + \gamma^3}\right)^{0.1}\right]^{-10} \end{array} \right\}^{-0.1}
\end{aligned}
\tag{4}
$$

where $\chi = H/P$ and $\gamma = H/T_s$. A comparison of Eq. (4) with the non-dimensional head/discharge curve by considering the developed crest length L highlights a decrease of the crest efficiency, because C_{dL} becomes less and less important with increasing head, while the efficiency of a linear weir always increases (Fig. 9). This phenomenon was also observed in trapezoidal labyrinth weirs with an influence of the angle α between the lateral crest and the main flow direction (Tullis *et al.* 1995), with $\alpha = 0$ for the PKW. For labyrinth weirs, the smaller α, the more important is the decrease of C_d with head. However, small α values cause an increase of L/W. The global
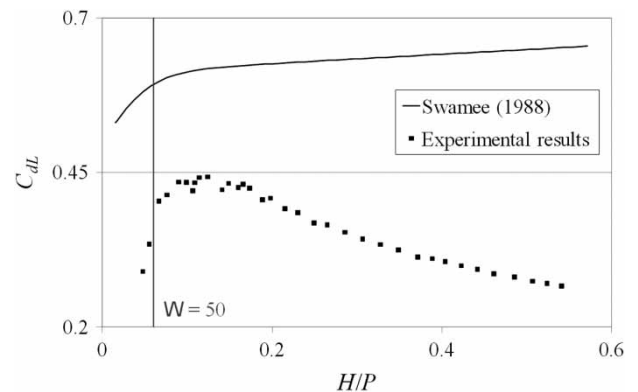

Figure 9　Comparison between crest efficiencies of tested model and linear weir, (vertical line|) limit of surface tension effects $W = 50$
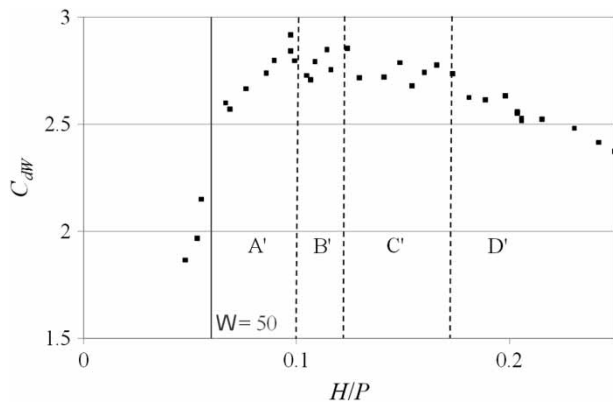
Figure 10   Discharge coefficient C_{dW} for low heads with A′ leaping nappe, B′ springing nappe on the lateral crest, C′ springing nappe on lateral and downstream crests, D′ springing nappe all over the crest, (|) limit of surface tension effects $W = 50$

weir efficiency, characterized by C_{dW}, increases thus with a decrease of α (Crookston and Tullis 2010).

For $H/P < 0.06$, surface tension effects on the PKW model excluded to determine the discharge capacity. From leaping to springing nappe flows, the discharge coefficient increases with the head as the crest efficiency increases (Fig. 10, region A′). For $H/P > 0.1$, springing nappe flow appears on 3/4 length of the lateral crest, and C_d is almost constant with increasing head (Fig. 10, region B′) because of the combined effects of decrease of the lateral crest efficiency due to its orientation ($\alpha = 0$), the efficiency increases due to leaping nappe flow on the downstream crest and clinging nappe flow on the upstream crest. If the downstream nappe becomes springing (Fig. 10, region C′), C_d decreases continuously with increasing head because of a small efficiency increase only due to clinging nappe flow on the upstream crest. Finally, C_d decreases further as the upstream nappe is free (Fig. 10, region D′).

The continuous decrease of C_d under increasing head according to Fig. 10 is explained by the streamline distribution under high heads. For these, the downstream inlet crest is over-supplied because of flow inertia in the downstream direction. More discharge than for low heads reach this section of the PKW. The lateral crest is poorly supplied because of the same longitudinal flow inertia. The streamline distribution along this crest is less dense. The upstream outlet crest is supplied equally for high and low heads (same streamlines).

A critical flow section advances from the downstream crest to the inlet for increasing heads generating an undular free surface downstream of the critical section. Because of the inlet slope and the associated flow depth variations, the streamlines converge along the inlet. The recirculation zones along the inlet side walls increase this phenomenon. Their sizes increase with the upstream head, reducing the effective inlet width. This cross-sectional reduction causes streamline concentration and so flow velocities in the axis of the inlet entrance (Fig. 8). As velocities increase the flow becomes supercritical, with the Froude number $F = U/(gh)^{1/2} > 1$, in which g is the acceleration of
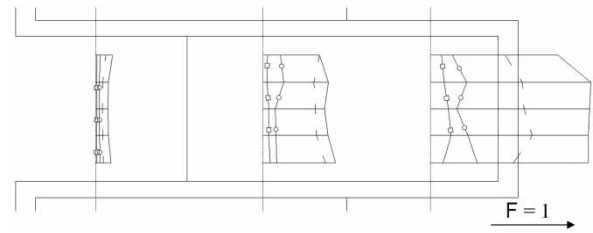

Figure 11   Froude number F profiles over PKW for $H/P = (-)\ 0.5$, $(-)\ 0.35$, $(-\bigcirc-)\ 0.2$, $(-\square-)\ 0.1$

gravity, h the flow depth and U the flow velocity (Fig. 11). The control section moves upstream with rising head, where the flow depth is larger. The effective weir length, and thus C_d decrease (Fig. 4 region A). For high heads, the control section is located at the inlet entrance. The discharge coefficient then decreases less (Fig. 4, region B) and tends to a limit value.

These observations explain the interest of increasing the inlet width, as long as the outlet width is sufficient to avoid lateral crest submergence (Ouamane and Lempérière 2006a, Machiels *et al.* 2009a), the inlet slope or the inlet height, using e.g. a crest extension (Ouamane and Lempérière 2006a,b) to increase C_d. An increase of the inlet cross-section increases the head required for the formation of a control section. It also explains the hydraulic advantage of using only upstream overhangs (Ouamane and Lempérière 2006a), to reduce the inlet length and increases its slope, and so limits the effect of the control-section. The use of a non-rectangular front part shape of the upstream overhangs (Ouamane and Lempérière 2006b) decreases the recirculation zone size and therefore increases the discharge capacity.

5   Conclusions

To enhance the understanding of the flows over PKWs, a 1:10 scale model was model-tested to determine the flow features depending on the upstream head. The flow conditions were characterized in terms of specific discharge, velocity, pressure, flow depth and streamlines along the weir. The results confirm the appealing discharge capacity of these weirs. The configuration studied is up to three times more efficient than an ogee-crest weir, despite a poor geometry. The effect of wall thickness and weir shape on the discharge capacity, decreasing the discharge efficiency for low heads, is highlighted. The velocity profiles combined with streamlines reveal the limitation of the inlet discharge capacity for high heads because a control section is formed. The position of the control section along the inlet explains the reduction of the discharge coefficient with head, because of the decrease on the effective weir crest length.

These observations explain the results of former studies. To avoid the formation of a control section along the inlet, geometric optimizations were proposed such as to increase the inlet width, the weir height or the upstream overhang length. The improvement of the shape of the upstream overhangs also limits the

formation of a critical section by a better distribution of velocities over the inlet width. All these optimizations and all those which may help to avoid occurrence of a critical section thus improve the discharge capacity of PKWs.

Notation

B = lateral crest length
B_i = downstream overhang length
B_o = upstream overhang length
C_{dL} = discharge coefficient of crest
C_{dW} = discharge coefficient of weir
F = Froude number
g = acceleration of gravity
h = flow depth
H = energy head
L = crest length of PKW-element
N_u = number of PKW-elements
P = PKW height
Q = discharge
T_s = wall thickness
U = velocity
W = PKW width
W = Weber number
W_i = inlet width
W_o = outlet width
W_u = PKW-unit width
α = angle between lateral crest and main stream direction
γ = H/T_s ratio
ρ = water density
σ = surface tension
χ = H/P ratio

References

Bieri, M., Leite Ribeiro, M., Boillat, J.-L., Schleiss, A., Laugier, F., Delorme, F., Villard, J.-F. (2009). Réhabilitation de la capacité d'évacuation des crues: Intégration de «PK-Weirs» sur des barrages existants [Rehabilitation of floods discharge capacity: Integration of «PK-Weirs» on existing dams]. Proc. Colloque CFBR-SHF: *Dimensionnement et fonctionnement des évacuateurs de crues*. SHF, Paris [in French] (CD-Rom).

Blanc, P., Lempérière, F. (2001). Labyrinth spillways have a promising future. *Hydropower & Dams* 8(4), 129–131.

Capart, H., Sillen, X., Zech, Y. (1997). Numerical and experimental water transients in sewer pipes. *J. Hydraulic Res*. 35(5), 659–672.

CETMEF (2005). *Notice sur les déversoirs:* Synthèse des lois d'écoulement au droit des seuils et déversoirs [Report on weirs: Synthesis of flow formulations for weirs and spillways]. CETMEF, Compiègne F, 1-89 [in French].

Crookston, B., Tullis, B. (2010). Hydraulic performance of labyrinth weirs. Proc. Int. Junior Researcher and Engineer Workshop *Hydraulic Structures* Edinburgh UK (CD-Rom).

Erpicum, S., Machiels, O., Archambeau, P., Dewals, B.J., Pirotton, M. (2010). 1D numerical approach to model the flow over a Piano Key Weir. Proc. *SimHydro* 2010 Nice. SHF, Paris (CD-Rom).

Fraccarollo, L., Toro, E.F. (1995). Experimental and numerical assessment of the shallow water model for two-dimensional dam-break type problems. *J. Hydraulic Res*. 33(6), 843–864.

Hien, T.C., Son, H.T., Khanh, M.H.T. (2006). Results of some piano keys weir hydraulic model tests in Vietnam. Proc. 22nd *ICOLD Congress*, Barcelona Q87(R39), 581–596.

Johnson, M.C. (2000). Discharge coefficient analysis for flat-topped and sharp-crested weirs. *Irrigation Science* 19(3), 133–137.

Klopfenstein, R., Jr. (1998). Air velocity and flow measurement using a Pitot tube. *ISA Trans*. 37(4), 257–263.

Laugier, F. (2007). Design and construction of the first Piano Key Weir spillway at the Goulours Dam. *Hydropower & Dams* 14(5), 94–101.

Laugier, F., Lochu, A., Gille, C., Leite Ribeiro, M., Boillat, J.-L. (2009). Design and construction of a labyrinth PKW spillway at Saint-Marc Dam, France. *Hydropower & Dams* 16(5), 100–107.

Le Doucen, O., Leite Ribeiro, M., Boillat, J.-L., Schleiss, A., Laugier, F. (2009). Etude paramétrique de la capacité des PK-weirs [Parametric study of PK-weir capacity]. Proc. *Modèles physiques hydrauliques*: Outils indispensables du XXIe siècle, Lyon, 155–160.SHF, Paris [in French].

Leite Ribeiro, M., Albalat, C., Boillat, J.-L., Schleiss, A.J., Laugier, F. (2007). Rehabilitation of St-Marc Dam: Experimental optimization of a piano key weir. Proc. 32nd *IAHR Congress*, Venice, (683) (CD-Rom).

Lempérière, F., Ouamane, A. (2003). The piano keys weir: A new cost-effective solution for spillways. *Hydropower & Dams* 10(5), 144–149.

Luck, M., Lee, E.-S., Mechitoua, N., Violeau, D., Laugier, F., Blancher, B., Guyot, G. (2009). Modélisations physique et numérique 3D pour l'évaluation de la débitance et le design des évacuateurs de crue [Physical and 3D numerical modeling for discharge calculation and design of weirs]. Proc. *Modèles physiques hydrauliques*: Outils indispensables du XXIe siècle, Lyon, 51–60. SHF, Paris [in French].

Machiels, O., Erpicum, S., Archambeau, P., Dewals, B.J., Pirotton, M. (2009a). Analyse expérimentale du fonctionnement hydraulique des déversoirs en touches de piano [Physical analysis of the hydraulic behavior of Piano Key Weirs]. Proc. Colloque CFBR-SHF. *Dimensionnement et fonctionnement des évacuateurs de crues*, SHF, Paris [in French] (CD-Rom).

Machiels, O., Erpicum, S., Archambeau, P., Dewals, B.J., Pirotton, M. (2009b). Large scale experimental study of piano key

weirs. Proc. 33rd *IAHR Congress*, Vancouver, 1030–1037 (CD-Rom).

Machiels, O., Erpicum, S., Archambeau, P., Dewals, B.J., Pirotton, M. ed. (2010). Piano Key Weirs: Experimental study of an efficient solution for rehabilitation, Proc. *FRIAR*, 95–106. Wessex Institute of Technology, Milano I.

Muste, M., Meselhe, E.A., Weber, L.J., Bradley, A.A. (2001). Coupled physical-numerical analysis of flows in natural waterways. *J. Hydraulic Res*. 39(1), 51–60.

Novak, P., Moffat, A.I.B., Nalluri, C., Narayanan, R. (1990). *Hydraulic structures*, Unwin Hyman, London, UK.

Ouamane, A., Lempérière, F. (2006a). Design of a new economic shape of weir. Proc. Int. Symp. *Dams in the Societies of the 21st Century*, Barcelona, 463–470.

Ouamane, A., Lempérière, F. (2006b). Nouvelle conception de déversoir pour l'accroissement de la capacité des retenues des barrages [New weir conception to increase dam reservoir capacities]. Proc. Coll. Int. *Protection et Préservation des Ressources en Eau*, Blida, Algérie, 59–67 [in French].

Pralong, J., Vermeulen, J., Laugier, F., Erpicum, S., Boillat, J.-L. (2011). A naming convention for the Piano Key Weir geometrical parameters. *Proc. Int. Workshop* Labyrinth and Piano Key Weirs *Liège B, 256–263*.

Swamee, P.K. (1988). Generalized rectangular weir equations. *J. Hydraulic Eng*. 114(8), 945–949.

Tullis, J.P., Amanian, N., Waldron, D. (1995). Design of labyrinth spillways. *J. Hydraulic Eng*. 121(3), 247–255.